IEEE Photonics Journal
An IEEE Photonics Society Publication

High-Speed Correlation and Equalization Using a Continuously Tunable All-Optical Tapped Delay Line

Volume 4, Number 4, August 2012

Salman Khaleghi, Student Member, IEEE
Omer F. Yilmaz, Member, IEEE
Mohammad Reza Chitgarha, Student Member, IEEE
Moshe Tur, Fellow, IEEE
Nisar Ahmed, Student Member, IEEE
Scott R. Nuccio, Member, IEEE
Irfan M. Fazal, Member, IEEE
Xiaoxia Wu, Member, IEEE
Michael W. Haney, Member, IEEE
Carsten Langrock
Martin M. Fejer, Fellow, IEEE
Alan E. Willner, Fellow, IEEE

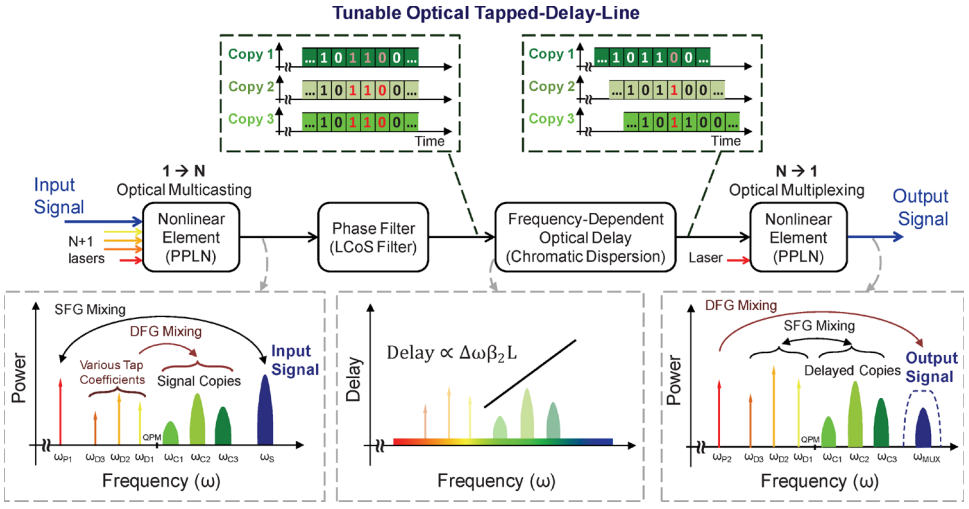

DOI: 10.1109/JPHOT.2012.2205671
1943-0655/$31.00 ©2012 IEEE

High-Speed Correlation and Equalization Using a Continuously Tunable All-Optical Tapped Delay Line

Salman Khaleghi,[1] *Student Member, IEEE*, Omer F. Yilmaz,[1] *Member, IEEE*, Mohammad Reza Chitgarha,[1] *Student Member, IEEE*, Moshe Tur,[2] *Fellow, IEEE*, Nisar Ahmed,[1] *Student Member, IEEE*, Scott R. Nuccio,[1] *Member, IEEE*, Irfan M. Fazal,[1] *Member, IEEE*, Xiaoxia Wu,[1] *Member, IEEE*, Michael W. Haney,[3] *Member, IEEE*, Carsten Langrock,[4] Martin M. Fejer,[4] *Fellow, IEEE*, and Alan E. Willner,[1] *Fellow, IEEE*

[1]Department of Electrical Engineering, University of Southern California, Los Angeles, CA 90089 USA
[2]School of Electrical Engineering, Tel Aviv University, Ramat Aviv 69978, Israel
[3]Department of Electrical and Computer Engineering, University of Delaware, Newark 19716 USA
[4]Edward L. Ginzton Laboratory, Stanford University, Stanford, CA 94305 USA

DOI: 10.1109/JPHOT.2012.2205671

Manuscript received June 12, 2012; accepted June 19, 2012. Date of publication June 22, 2012; date of current version July 16, 2012. This work was supported by the Defense Advanced Research Projects Agency (DARPA) under Contract numbers N00014-05-1-0053, W911NF-10-1-0151, and FA8650-08-1-7820. This paper was presented in part at the Optical Fiber Communication Conference (OFC) and the European Conference on Optical Communications (ECOC). S. Khaleghi and O. Yilmaz contributed equally. Co-corresponding authors: S. Khaleghi and O. Yilmaz (e-mail: khaleghi@usc.edu; oyilmaz@usc.edu).

Abstract: We demonstrate a reconfigurable high-speed optical tapped delay line (TDL), enabling several fundamental real-time signal processing functions such as correlation (for pattern search) and equalization. Weighted taps are created and added using optical multicasting and multiplexing schemes that utilize the nonlinear wave mixings in the periodically poled lithium niobate (PPLN) waveguides. Tunable tap delays are realized using the conversion–dispersion technique. In the demonstrated TDL, the amplitude and phase of tap coefficients can be varied, enabling signal processing on amplitude- and phase-encoded optical signals. We experimentally demonstrate the tunability of the TDL in time, amplitude, and phase. We analyze the TDL's theory of operation and present experimental results on reconfigurable pattern search (correlation) on on–off-keyed and phase-shift-keyed signals at data rates of up to 80 Gb/s, as well as equalization for chromatic dispersion.

Index Terms: Fiber optics links and subsystems, all-optical correlation, equalization, nonlinear wave mixing, wavelength conversion, dispersion, optical signal processing.

1. Introduction

High-data-rate all-optical signal processing has been one of the main research goals in photonics. Signal processing using nonlinear optics has been of great interest due to its inherent ultrafast THz bandwidth and its potentially phase-preserving nature [1]–[3]. Many important functions for signal processing have been implemented using various forms of photonic nonlinear interactions [4]–[6]. Future optical signal processing systems can benefit from nonlinear optics for wavelength conversion [5], add–drop multiplexing of digital signals [6], and quantization [4]. A key building block of many digital signal processing applications is the tapped

delay line (TDL), in which an incoming data stream is tapped at different time intervals, given amplitude weights, and then added together [7]. A TDL can be configured to provide a variety of important signal processing functions, including i) finite-impulse response (FIR) filtering, ii) signal correlation and convolution, iii) digital-to-analog conversion, iv) equalization, and v) discrete Fourier transform (DFT) [7], [8].

In signal processing, TDLs have been implemented electronically, providing these key functions in a reconfigurable fashion but on the binary electrical signals [9]. Utilization of the extremely large bandwidth of photonic technologies would require implementation of TDLs all-optically. An optical method can potentially advance the performance of signal processing when the signal to be processed is at high speed or is a combination of many lower speed signals [10], [11]. The optical data signal flows through the TDL module without the need to actively operate/switch on each bit individually. Moreover, optical signal processing can also benefit from the ability to manipulate and process optical field amplitude and phase in order to increase the capacity and speed of processing. For optical TDLs, critical issues include the following abilities: a) continuously tune tap delays from a fraction of a bit time to multiple bit times, b) finely tune the relative tap delays since fractions of a bit time at tens of gigabaud can easily be on the order of a few picoseconds, and c) accommodate different data modulation formats [e.g., on–off keying (OOK) and phase-shift keying (PSK)].

Recent work on optical TDLs includes fixed fiber-based TDLs [12], cascaded Mach–Zehnder interferometers [10], [13], and hybrid optical and electrical approaches that take advantage of microwave photonics techniques [14], [15]. These approaches are generally fixed or are tunable over finite or discrete ranges, or tend not to have independent control over the amplitude, phase, and delay of each tap. We propose and demonstrate an optical TDL that utilizes recent advances in the fields of optical multicasting, multiplexing, and conversion–dispersion delays [16] to realize a tunable and reconfigurable optical TDL.

In this paper, we report a reconfigurable all-optical TDL that is continuously tunable in all aspects (amplitude, phase, delay, and number of the taps) and thus can be programmed in the field to perform a desired function (e.g., equalization or correlation). Our approach takes advantage of ultrafast optical nonlinear effects to create and combine the taps, as well as all-optical tunable conversion–dispersion-based delays. We show real-time optical equalization and correlation at line rates as high as 80 Gb/s using the optical TDL with two to four taps. We demonstrate TDL schemes with i) optical multiplexing (enabling processing of amplitude and phase) and ii) electronic multiplexing [for amplitude-modulated (OOK) signals]. The optically multiplexed TDL-based equalizer is used to compensate the chromatic dispersion (CD) on differential binary phase-shift-keyed (DPSK) and differential quadrature phase-shift-keyed (DQPSK) signals. An optical TDL equalizer with half a symbol time tap spacing is demonstrated at 40- and 27-GBd data rates. Optical TDL-based correlation for pattern detection has been realized to search for 3- and 4-symbols-long patterns in OOK, binary phase-shift-keyed (BPSK), and quadrature phase-shift-keyed (QPSK) signals. Electrical multiplexing is utilized to realize correlation and equalization with bipolar taps, resulting in an electrical output signal.

2. Concept and Principle: All-Optical TDL

The generic form of a tunable TDL is shown in Fig. 1. For a TDL with N taps, taken at times T_i, and weighted by complex coefficients $|h_i|\angle h_i$, the relation between the input signal $x(t)$ and the output $y(t)$ is determined by $y(t) = \sum_{k=0}^{N-1} h_i\, x(t - T_i)$. Therefore, the function of the TDL is simply controlled by the number of taps (N), the tap delays (T_i), and the complex tap coefficients (h_i).

The principle of operation of our proposed optical TDL is depicted in Fig. 2. First, a nonlinear optical mixer and multiple dummy tunable pump lasers can multicast (fan-out) N replicas of the data signal, with each replica located at a different center frequency. A liquid crystal on silicon (LCoS) programmable filter can be used to apply the tap phases. Subsequently, these replicas travel through a chromatic dispersive element at various speeds incurring a different time delay. Finally, these N replicas are multiplexed together by another high-speed nonlinear mixer creating an output signal that is "processed" by the TDL. The taps can be precisely tuned in terms of amplitude, phase, and relative time delay by varying the pump lasers.

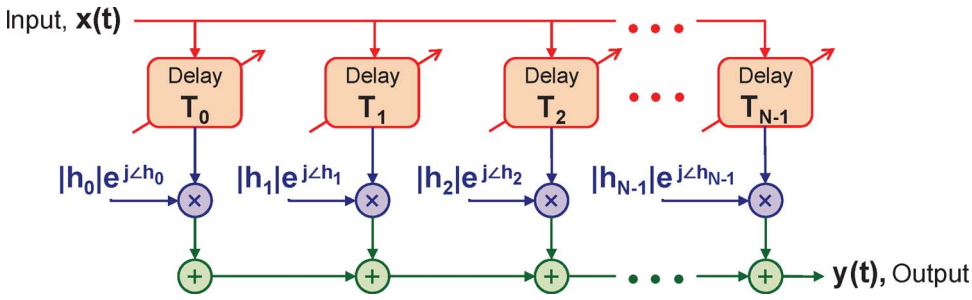

Fig. 1. Generic block diagram of a TDL: Input signal is tapped at different time intervals, taps (copies) are weighted each by its own coefficient and then summed to produce the output.

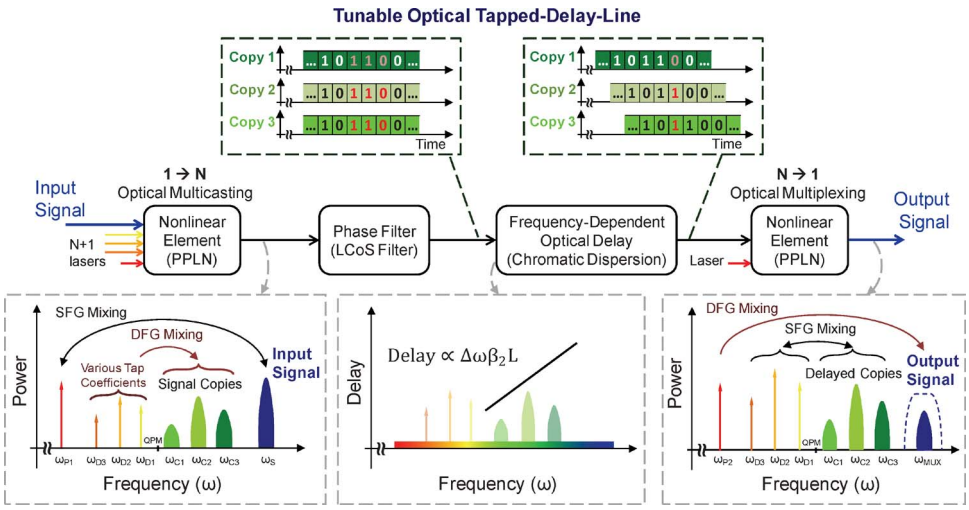

Fig. 2. Optical implementation of a TDL based on nonlinearities and conversion–dispersion-based delays: *N* copies of the input optical signal are generated at different frequencies using cascaded nonlinear wave mixings of SFG followed by DFG. The amplitude of each signal copy depends on its CW laser pump power. Copies are sent into a chromatic dispersive medium to introduce the tap delays. Delayed and weighted signal copies are sent to a second nonlinear medium to be multiplexed and create the output signal. $\Delta\omega$: Frequency separation between signal copies, β_2: Group velocity dispersion parameter, *L*: Length of the dispersive medium, PPLN: Periodically poled lithium niobate.

Various schemes have been used in the literature for multicasting, conversion–dispersion delays, and optical multiplexing. For optical multicasting, different media and nonlinearities have been utilized, including four-wave mixing (FWM) in semiconductor optical amplifiers (SOAs) [17], silica-based highly nonlinear fibers (HNLFs) [18], and silicon nanowires [19]. Cascaded sum-frequency generation followed by difference-frequency generation (cSFG–DFG) in periodically poled lithium niobate (PPLN) waveguides have also been used for multicasting [20].

We utilize chromatic-dispersion-based delays to realize tap delays [16], [21]–[23]. The chromatic-dispersion-based delays exploit the wavelength-dependent speed of light in a dispersive medium coupled with tunable wavelength conversion to achieve continuously tunable delays. Using HNLF for wavelength conversion, distortion-free 22-ns delay is demonstrated for 2.6-ps-wide optical signals [21], and 105-ns delay is shown for 10-Gb/s optical signals [22]. Conversion–dispersion delays have also been realized using PPLN waveguides as their wavelength converters [23]. Fine tuning resolution of < 500 fs is reported for conversion–dispersion-based optical delays [24].

Prior work on nonlinear optical multiplexing has been based on FWM [25], cross-phase modulation (XPM) [26], and supercontinuum generation [26], [27] in HNLFs. Cascaded SFG–DFG

processes in PPLN waveguides have also been used as the medium to time multiplex eight lower rate 20-Gb/s OOK signals to a 160-Gb/s signal [28], and add/drop multiplexing at 640-Gb/s data rates [6].

In our optical TDL approach, PPLN waveguides are chosen as the nonlinear optical wave mixer for multicasting (fan-out) and multiplexing stages. FWM interactions in HNLF fibers could produce extra mixing products that might be undesirable since they occupy bandwidth and could cause crosstalk. The wave mixing interactions (cSFG–DFG) are governed by conservation of energy and phase-matching conditions [29], as discussed in the following.

2.1. Optical Multicasting (Fan-Out)

In the fan-out stage, copies of an amplitude- and/or phase-encoded incoming signal (at ω_S) are generated using cSFG–DFG processes [1], [29]. The signal at ω_S and a continuous-wave (CW) pump laser at ω_{P1}, which are located symmetrically around the quasi-phase matching (QPM) frequency ω_{QPM} of the PPLN waveguide, mix through the SFG process to produce a signal copy at $\omega_S + \omega_{P1} = 2\omega_{QPM}$. The SFG term then mixes with multiple dummy pump lasers at frequencies ω_{Di} through the DFG nonlinear process to create signal copies at $2\omega_{QPM} - \omega_{Di}$. Thus, the generated output signal copies will be at frequencies $\omega_{Ci} = \omega_S + \omega_{P1} - \omega_{Di}$ (see Fig. 2, schematic spectrum on the left).

Given the electric field of the signal $A_S(t)$, CW DFG dummy pump lasers $A_{Di}(t)$, and the CW SFG pump laser $A_{P1}(t)$, the amplitude of the generated signal copy is $A_{Ci}(t) \propto A^*_{Di}A_{P1}A_S(t)$, in which A^*_{Di} denotes the complex conjugate of A_{Di}. Therefore, the amplitude of each signal copy is proportional to the amplitude of the dummy pump laser that generated it. Therefore, variable weight taps can be realized by varying the dummy lasers' powers.

2.2. Phase Tuning and Optical Delays

The signal copies and their corresponding dummy pumps are filtered and sent into an amplitude- and phase-programmable filter (based on LCoS technology [30]), in which i) the signal copies (ω_{Ci}'s) and their dummy pumps (ω_{Di}'s) are filtered, and ii) a phase shift ϕ_i^{LCoS} is applied to each dummy pump laser ω_{Di}, as depicted in Fig. 4. Eventually after multiplexing, these applied phases turn out to be the tap phases. The output is then sent into a dispersive medium of length L and propagation constant $\beta(\omega)$. Therefore, the fields of the delayed signal copies, $A_{DCi}(t)$, and the delayed dummy pumps, A_{DDi}, become:

$$A_{DCi}(t) \propto A^*_{Di}A_{P1}\Im^{-1}\left\{\widetilde{A_S}(\omega)e^{-j\beta(\omega)L}\right\} \tag{1}$$

$$A_{DDi} \propto A_{Di}e^{-j\beta(\omega_{Di})L}e^{j\phi_i^{LCoS}}. \tag{2}$$

In which $\widetilde{A_S}(\omega) = \Im\{A_S(t)\}$ is the Fourier transform of $A_S(t)$, $e^{-j\beta(\omega)L}$ is the transfer function of the dispersive medium at frequency ω, and $\omega_{Ci} = \omega_S + \omega_{Pi} - \omega_{Di} = 2\omega_{QPM} - \omega_{Di}$ is the frequency of the ith signal copy. The Taylor series expansion of $\beta(\omega)$ around ω_{QPM} gives $\beta(\omega) = \sum_{n=0}^{\infty}((\omega - \omega_{QPM})^n/n!)\beta_n$, in which $\beta_n = (\partial^n\beta/\partial\omega^n)|_{\omega=\omega_{QPM}}$; β_2 is known as the group velocity dispersion parameter [1]. According to the group delay, the signal copy at ω_{Ci} will be delayed by $T(\omega_{Ci}) = L(\partial\beta/\partial\omega)|_{\omega=\omega_{C_i}}$. If higher order dispersion parameters are negligible (i.e., $\beta_j \approx 0$ for $j \geq 3$), the group delay at frequency ω_{Ci} becomes $T(\omega_{Ci}) \approx \beta_1 L + (\omega_{Ci} - \omega_{QPM})\beta_2 L$. Therefore, the relative delay on each signal copy compared with the first copy $A_{DC1}(t)$ is $T_i = T(\omega_{Ci}) - T(\omega_{C1}) = (\omega_{D1} - \omega_{Di})\beta_2 L$. Thus, if phase-constant terms are ignored, the fields of the delayed copies are proportional to $A_{DCi}(t) \propto A^*_{Di}A_{P1}A_S(t - T_i)$, assuming negligible signal distortion due to the dispersion. As shown in Fig. 2, after passing through a dispersive medium [e.g., dispersion compensating fiber (DCF)], the signal copies are relatively delayed with respect to each other. These tap delays are proportional to the frequency spacing between the signal copies and can be tuned by changing the signal copy frequencies ω_{Ci}'s (or equivalently, ω_{Di}'s).

2.3. Optical Multiplexing

Similar to the optical multicasting stage, cSFG–DFG processes are used in another PPLN waveguide with the same QPM frequency ω_{QPM} as the first PPLN waveguide for optical multiplexing. As depicted in Figs. 2 and 4, the signal copies at ω_{Ci}'s and their dummy pumps ω_{Di}'s are kept and reused for phase-preserving multiplexing. In the multiplexing stage, each delayed signal copy ω_{Ci} mixes with its reused dummy pump ω_{Di} through SFG and creates a signal at $\omega_{Ci}+\omega_{Di}=2\omega_{QPM}$. Another pump laser at ω_{P2} is also injected to the second PPLN waveguide for the DFG process to convert this signal to frequency $\omega_{MUX}\triangleq 2\omega_{QPM}-\omega_{P2}=\omega_{Ci}+\omega_{Di}-\omega_{P2}$. After the second PPLN waveguide, the field of the ith multiplexed copy is $A_{MUXi}(t)\propto A_{P_2}^{*}A_{DDi}A_{DCi}(t)$, or:

$$A_{MUX_i}(t)\propto A_{P_2}^{*}A_{P_1}|A_{D_i}|^2 e^{j\Phi_i}e^{j\phi_i^{LCoS}}A_S(t-T_i). \tag{3}$$

In which $\Phi_i\triangleq -L\beta(\omega_{Di})-L\beta(\omega_{Ci})$. Because of the symmetry around ω_{QPM} (i.e., $\omega_{QPM}-\omega_{Di}=\omega_{Ci}-\omega_{QPM}$), the Taylor series expansion of Φ_i only includes even terms as shown in

$$\begin{aligned}\Phi_i &= -\sum_{n=0}^{\infty}\frac{(\omega_{Di}-\omega_{QPM})^n}{n!}L\beta_n-\sum_{n=0}^{\infty}\frac{(\omega_{Ci}-\omega_{QPM})^n}{n!}L\beta_n\\ &= -2L\beta_0-(\omega_{Di}-\omega_{QPM})^2L\beta_2-\ldots.\end{aligned} \tag{4}$$

Furthermore, Φ_i of a tap only depends on its parent's dummy pump laser frequency ω_{Di}. Assuming negligible fourth-order and higher order dispersion (i.e., $\beta_j\approx 0$ for $j\geq 4$) and ignoring constant phase terms, $\Phi_i\approx -(\omega_{Di}-\omega_{QPM})^2L\beta_2\triangleq\Phi_i^{initial}$. The total multiplexed signal is expressed by $A_{MUX}(t)=\sum_{i=1}^{N}A_{MUXi}(t)$, or:

$$A_{MUX}(t)\propto\sum_{i=1}^{N}e^{j\Phi_i^{initial}}|A_{Di}|^2e^{j\left(\phi_i^{LCoS}\right)}A_S(t-T_i). \tag{5}$$

This is equivalent to a TDL with input $A_S(t)$, output $A_{MUX}(t)$, and input–output relation

$$A_{MUX}(t)\propto\sum_{i=1}^{N}|h_i|e^{j\angle h_i}A_S(t-T_i). \tag{6}$$

In which:

$$\begin{aligned}|h_i| &= |A_{D_i}|^2\\ \angle h_i &= \Phi_i^{initial}+\phi_i^{LCoS}\\ T_i &= L\ \beta_2\ (\omega_{Di}-\omega_{D1})\\ \Phi_i^{initial} &= -\ L\ \beta_2(\omega_{Di}-\omega_{QPM})^2.\end{aligned} \tag{7}$$

According to (7), each tap is generated by a dummy pump laser (at ω_{Di}). Therefore, the number of taps (N) can be changed by adding/removing dummy pump lasers, and the amplitude of each tap $(|h_i|)$ can be varied independently by adjusting its dummy pump laser power $(|A_{Di}|^2)$ in the optical fan-out stage. Also, the delay of each tap (T_i) can be varied by changing the dummy pump laser frequency (ω_{Di}). The challenge in realizing phase tuning lies in the fact that the generated signal copies need to be phase coherent before they can be multiplexed. In our approach, the dummy pumps are kept on the same optical path along with their corresponding signal copies to preserve phase coherence and enable phase tuning of taps. The relative phase of each replica $(\angle h_i)$ can be tightly controlled by applying a phase shift using an LCoS filter (ϕ_i^{LCoS}) or fine detuning to the frequency of dummy lasers. A fine detuning of $\delta\omega_{Di}$ changes $\Phi_i^{initial}$ by $\delta\phi_i\approx -2L\beta_2(\omega_{Di}-\omega_{QPM})\delta\omega_{Di}$. However, the pump detuning changes the tap delays by $\sim L\beta_2\delta\omega_{Di}$. For system designs in which this delay offset is negligible compared with the tap delays, the tap phases can be applied directly by

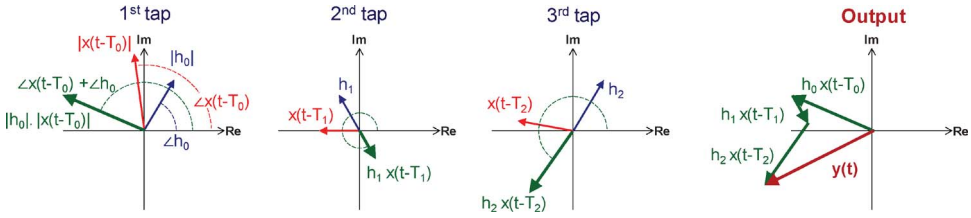

Fig. 3. Mathematical vector representation of TDL operation. In each tap, the delayed input is multiplied by a complex coefficient that could rotate and scale it. The output y(t) is a vector summation of the weighted taps.

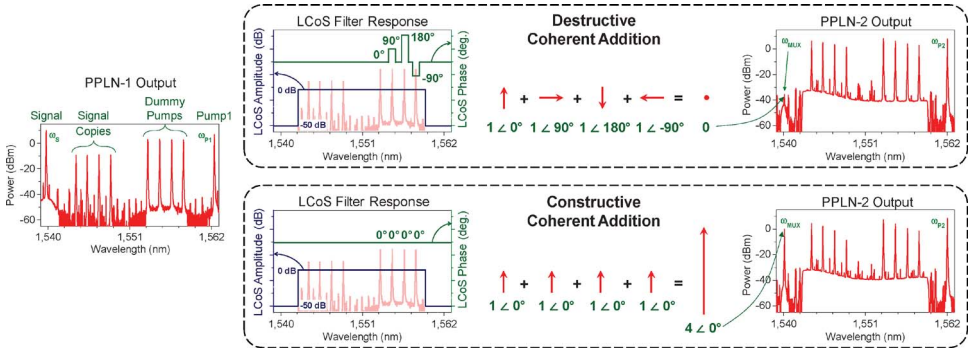

Fig. 4. Measured spectrum of the output of the fan-out stage (PPLN-1) with four taps, in which the signal is constant (CW pump laser). Schematic LCoS filter responses, showing tap phase tuning. Output spectra of the multiplexing stage (PPLN-2) when phases of the tap coefficients result in destructive (right top) and constructive (right bottom) addition of taps.

detuning the dummy pumps. In either case, the phases $\Phi_i^{initial}$ associated with the pumps located at ω_{Di} need to be added to the desired tap phases to initialize the system.

Fig. 3 illustrates how complex tap coefficients can rotate and scale input symbols (vectors) in the complex plane and produce the TDL output by a vector addition. Fig. 4 explains the principle of coherent addition on a constant input signal (i.e., a CW laser). Four equal-amplitude taps are used (as shown in PPLN-1 output), and depending on the phases of tap coefficients (applied by the LCoS filter), these four copies can be added constructively or destructively, resulting in either a high-power peak or a low-power null at ω_{MUX} (PPLN-2 output).

As an alternative to optical multiplexing, the taps can be electronically combined in a photodiode, provided that the beating terms between different wavelength channels fall outside the bandwidth of the photodiode. Photodiodes detect the intensity of light, which is a positive quantity; therefore, if a balanced photodiode (BPD) is used, bipolar (negative and positive) tap coefficients can be realized.

The TDL can be utilized for many different applications by programming the tap delays, amplitudes, and phases [31]–[33]. In the following sections, we demonstrate two different applications: i) pattern correlation for both amplitude- and phase-encoded signals [31], [32] and ii) equalization of CD [31], [33].

3. Experimental Setup

The experimental setup for the all-optical TDL is shown in Fig. 5. Also, shown in Fig. 5 are sample measured spectra after the first and second PPLN waveguides for a three-tap TDL with different tap amplitudes. After optical wavelength multicasting (fan-out) and dispersive medium, the taps (signal copies) can be combined using either optical multiplexing or electrical multiplexing (in photodiodes). In the latter, the input signal is optical, and the output is a bipolar electrical signal.

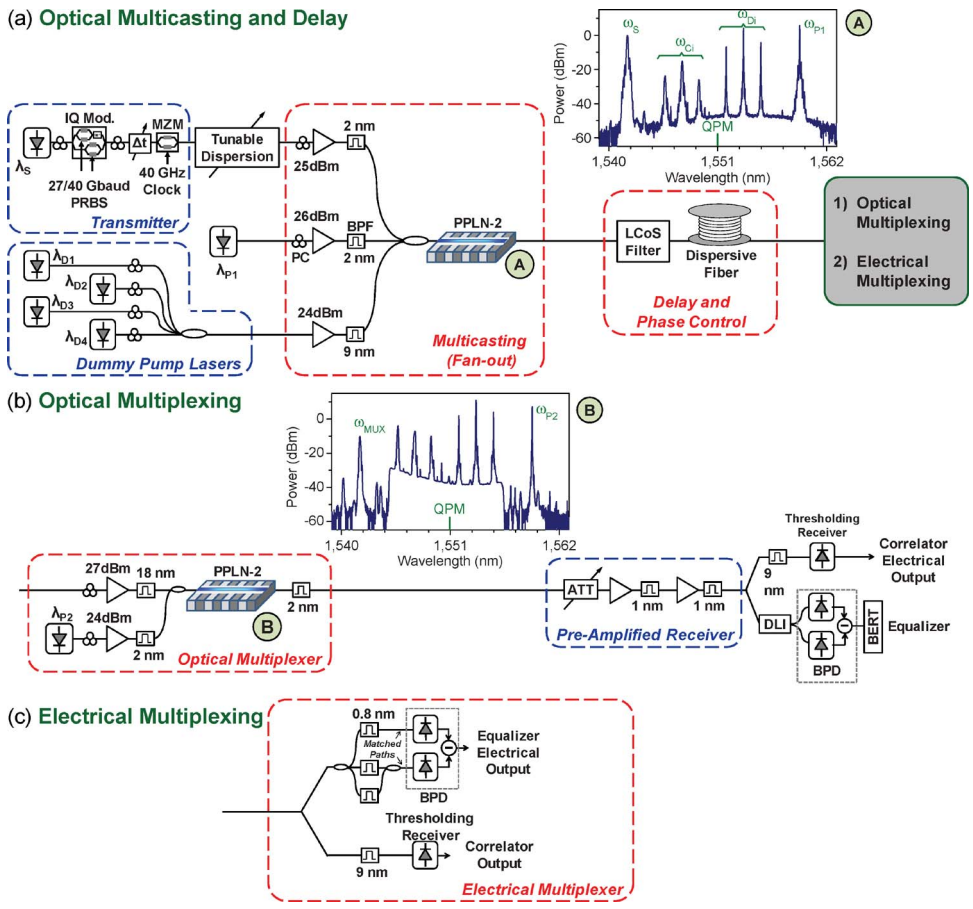

Fig. 5. Experimental setup for an optical TDL for equalization and correlation. (a) Multicasting and delay, (b) optical multiplexing, and (c) electrical multiplexing. Spectra of the first and the second PPLN waveguide outputs are shown for a three-tap optical TDL with various tap amplitudes. PPLN: Periodically poled lithium niobate waveguide, LCoS: liquid crystal on silicon, PC: polarization controller, BPF: bandpass filter, ATT: attenuator, DLI: delay-line interferometer, BERT: bit-error-rate tester, BPD: balanced photodiode, MZM: Mach–Zehnder modulator.

3.1. Complex-Coefficient TDL Using Optical Multiplexing

As depicted in Fig. 5, for equalization and correlation experiments 27/40-Gb/s NRZ-BPSK and NRZ-DPSK signals, 62/80-Gb/s NRZ-QPSK and NRZ-DQPSK signals were generated using a CW laser at wavelength $\lambda_S \sim 1539.3$ nm and nested Mach–Zehnder modulators (MZMs). The 40-Gb/s OOK signal was generated using an MZM symmetrically driven around $V_\pi/2$. To generate 50% RZ waveforms for 40-GBd signals, another MZM was cascaded as a pulse carver and was driven by a 40-GHz clock signal. Pseudo-random bit sequence (PRBS) $2^{31}-1$ was used for the equalization experiments, whereas a PRBS 2^7-1 pattern was chosen for the correlation results (to show a 127-bit-long waveform). For the equalization experiments, a fiber-Bragg-grating-based tunable dispersion compensating module (TDCM) emulated CD to distort the input signal.

The signal was coupled with a CW pump ($\lambda_{P1} \sim 1562.1$ nm, for the SFG process) and four tunable CW lasers (λ_{D1-4} :$\sim 1553.6- \sim 1558.4$ nm for DFG processes) and sent to the first PPLN waveguide, in which the QPM wavelength is temperature tuned to 1550.7 nm. The signal and λ_{P1} pump powers were $\sim$80 mW, and each dummy pump power launched into the first PPLN waveguide was $\sim$35 mW. The CW pump lasers (λ_{D1-4}) generated the signal copies (λ_{C1-4}). The signal copies and corresponding pump lasers were all filtered using an amplitude- and phase-programmable filter based on LCoS technology and sent to a DCF to introduce tap delays. The fiber CD D is related to the group velocity dispersion parameter according to $D \approx -2\pi c\beta_2/\lambda^2$, in which c

is the speed of light [1]. Therefore, a DCF of length L induces a relative delay of $\Delta t = D \times L \times \Delta\lambda$ between two signals with wavelength separation of $\Delta\lambda$. DCF lengths of 90 and 180 m were used in equalization and correlation experiments, respectively. The DCF has $D \approx -86$ ps/nm/km dispersion. For 1.6-nm wavelength separation, this corresponds to ~12.5-ps and ~25-ps delay after 90- and 180-m DCF spools, respectively. In TDL, delays from a fraction of a symbol time to few symbol times between the taps would be desirable. For 40-GBd signals, the delays would be in a picosecond range, and thus, realizing them may not require the complexity of very large conversion–dispersion delays [21], including dispersion compensation. The use of DCF can inherently distort the signals through the TDL; however, for short delays where the DCF is relatively small, dispersion compensation may not be necessary on the output of the TDL. Moreover, to keep unwanted mixing terms low, the launch powers and the wavelength spacing between the dummy pumps, the signal, and the QPM wavelength are chosen with care.

When filtering the signal copies and dummy pumps, the LCoS programmable filter also applied the tap phases on the dummy pumps. After the DCF, the dummy pumps and copies were amplified, and then filtered with a center- and bandwidth-tunable filter of 15-nm maximum bandwidth. The output was coupled with a CW pump laser at λ_{P2} and sent to a second PPLN waveguide for optical multiplexing. For DFG mixing in the second PPLN waveguide, a CW pump laser $\lambda_{P2} \sim 1562.1$ nm was used. Alternatively, the pump laser λ_{P1} can also be split and used in both the first and second stages. The power launched into the second PPLN waveguide was ~90 mW for λ_{P2} pump plus ~200 mW for all signal copies and their reused dummy pumps. The QPM wavelength of the second PPLN waveguide was temperature tuned to 1550.7 nm as well. The first and second PPLN waveguides were 4 and 5 cm long, respectively. The multiplexed signal was generated at 1539.3-nm wavelength and was filtered and sent to a preamplified receiver. Single-ended and BPDs with 30-GHz bandwidth were used for direct detection in the equalizer experiments. Bit-error-rate (BER) measurements are performed on the equalized output of the TDL. A thresholding balanced photoreceiver was used for electrical thresholding of the optical correlation waveforms to distinguish the full match from partial matches.

3.2. Bipolar-Coefficient TDL Using Electrical Multiplexing

A 40-Gb/s NRZ-OOK signal $(\lambda_S \sim 1549.4\ \text{nm})$ is generated using an MZM driven by a $2^{31} - 1$ PRBS. An amplified spontaneous emission (ASE) noise source along with an attenuator is used to noise load the transmit signal in order to change the input optical signal-to-noise ratio (OSNR). The data signal is coupled with a second pump $(\lambda_{P1} \sim 1553.4\ \text{nm})$ and four tunable CW lasers (λ_{D1} to λ_{D4}) and is sent into a 5-cm-long PPLN waveguide with a temperature-tuned QPM wavelength of 1551.4 nm. All pumps and data signal are amplified and filtered before the PPLN waveguide to enhance wavelength conversion efficiency and the OSNR. The four pump lasers (λ_{D1} to λ_{D4}) allow for realization of four taps (λ_{C1} to λ_{C4}). For the intensity-based correlator, equal tap weights are used, while the tap weights for the three-tap equalizer are tuned for optimal equalization performance by adjusting the respective CW powers. The multicast signals are then filtered by a 9-nm filter and sent to a dispersive medium in order to induce a wavelength-dependent delay. A ~1-km single-mode fiber (SMF) is used for the correlator, where a ~60-m DCF is used for the equalizer experiments with electrical multiplexing. For the correlator, the delayed signal copies are then sent to a ~30-GHz bandwidth thresholding receiver in order to find the correlation peaks. Because an equalizer requires bipolar tap weights, all positive taps are multiplexed in the positive port of a BPD, and all negative taps are multiplexed on its negative port. A ~36-GHz BPD is utilized for this purpose. Positive and negative taps are first filtered separately by 0.8-nm BPFs and are then combined together and sent to the BPD, as shown in Fig. 5. The fiber lengths are matched for the positive and negative taps prior to the BPD. An equalized electrical signal is achieved at the output of the BPD, which is sent to the BER measurement system.

4. Correlation and Pattern Recognition

The optical TDL could be programmed to search and recognize a specific pattern on a data stream [8], [13]. A high-speed pattern search to locate and identify features of interest is very desirable in

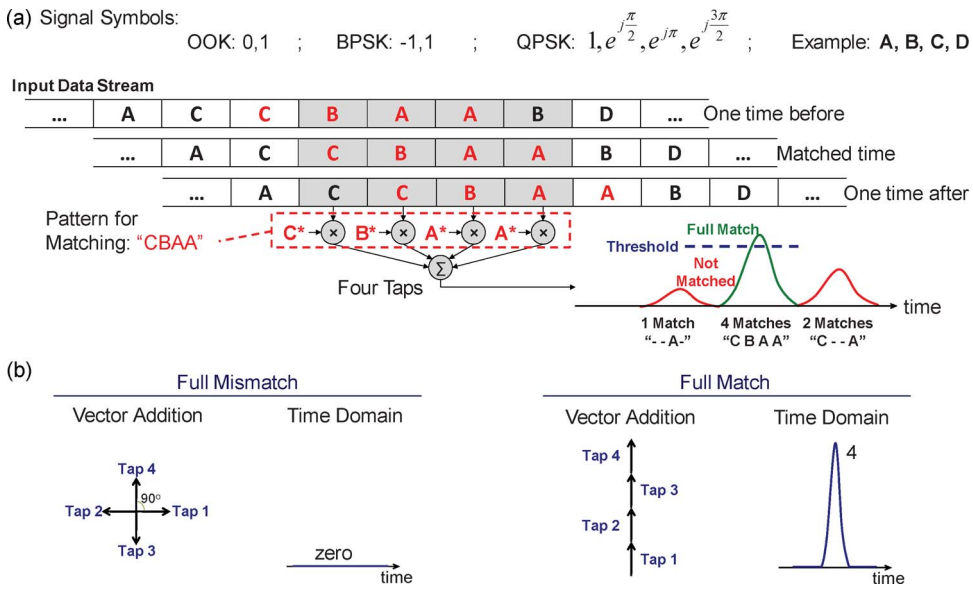

Fig. 6. Concept of a TDL-based correlator. (a) TDL coefficients are determined by the search pattern. Input data stream slides through the TDL resulting in a high correlation peak when full pattern matching occurs. (b) Complex-coefficient taps allow for vector addition of adjacent symbols to create correlation peaks, enabling correlation on PSK signals.

different fields of science, especially for searching large amounts of data. A correlator can perform pattern recognition and detect the location of a predetermined pattern in a data set. Fig. 6 shows the concept of pattern matching using a correlator. Generally in correlators, a data stream slides through a set of taps. These taps basically multiply adjacent data symbols by various tap coefficients. The tap coefficients represent the pattern that we intend to match to. After the adjacent symbols (taps) are multiplied by a complex coefficient, they are added to form the output. Fig. 6(b) illustrates through the vector addition concept the generation of a correlation peak when patterns fully match.

4.1. Correlation Using Optical Multiplexing

The correlator in Fig. 6(a) operates on {A, B, C, D} symbols. The search pattern is "C B A A"; therefore, its complex conjugate is applied on the tap coefficients. As the input data slide through the correlator, if all four adjacent symbols on the input match the search pattern, the correlator will output a full four-level signal [middle peak in Fig. 6(a) output]. However, if there is an in-exact match between the sliding data stream and the pattern (tap coefficients), the correlator output will have a lower amplitude. Therefore, a thresholder can be used after the correlator to detect this maximum peak and simply determine "when and where" a pattern is found in the data steam and to what extent a pattern is matched.

As illustrated in Fig. 6(a), to recognize a phase/amplitude pattern of length *N*, a TDL with *N* taps located at one-symbol-time intervals is required. Moreover, the tap coefficients need to be set equal to the complex conjugate of the target pattern [32]. If the TDL allows for complex tap coefficients, patterns can be searched in the multilevel PSK signals. Fig. 7 shows sample experimental results for correlators operating on OOK, BPSK, and QPSK signals at different bit rates and different target patterns. For each signal, the spectra of the nonlinear wave mixing for multicasting stage and multiplexing stages are shown, as well as the output eye diagram and optical output waveform (intensity after photodiode) and electrically thresholded waveform (electrical output of the thresholding photoreceiver). The target search pattern in the correlator is controlled by the pump wavelengths (delays) and the relative phases of each idler. In Fig. 7(a), correlation results are presented for searching a 4-bit amplitude pattern "1 1 1 1" in 40-Gb/s RZ-OOK signals. Fig. 7(b)

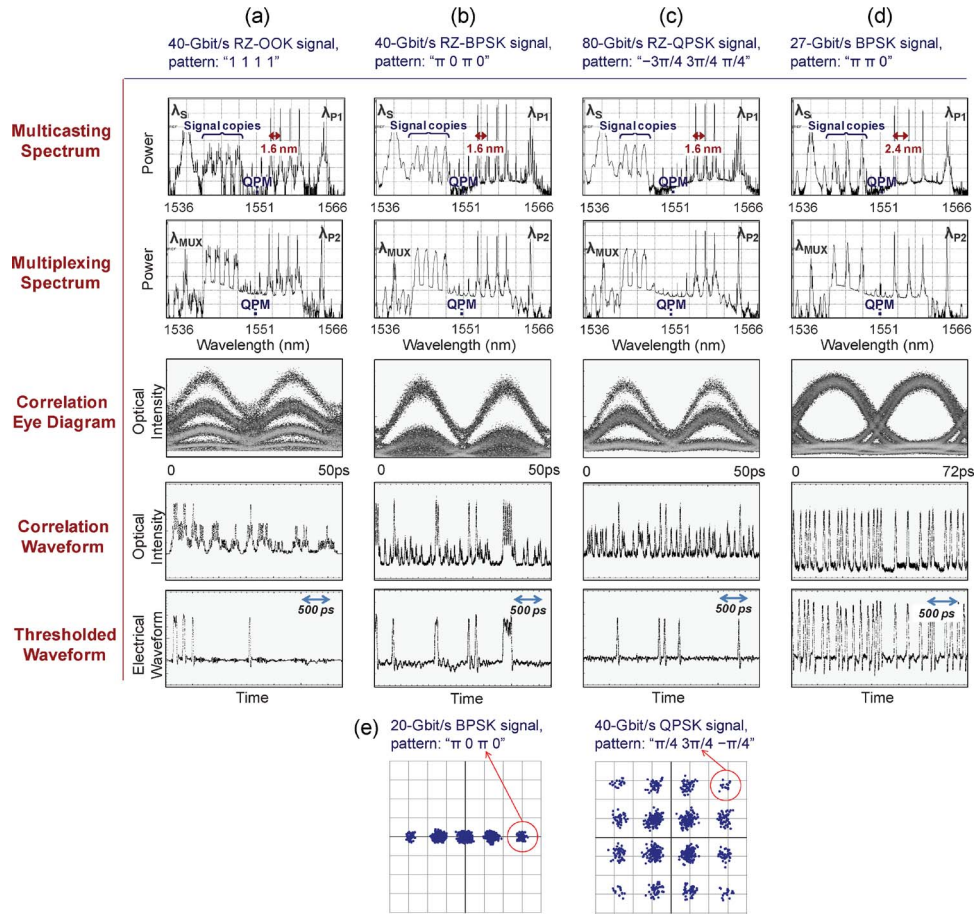

Fig. 7. All-optical TDL correlation results for (a) 40-Gb/s OOK, (b) 40-Gb/s BPSK, (c) 80-Gb/s QPSK, and (d) 27-Gb/s BPSK signals. (e) Coherent detection of 20-GBd BPSK and QPSK correlator output.

shows results on a 40-Gb/s RZ-BPSK signal where target phase pattern is "π 0 π 0". For an 80-Gb/s QPSK signal, a length-three phase pattern "$-3\pi/4$ $3\pi/4$ $\pi/4$" is searched using three dummy pumps in Fig. 7(c). For 40-GBd signals, the wavelength separations between dummy pumps are set to $\sim$1.6 nm, which is equivalent to 25-ps delay (one symbol time) between the taps after passing through the DCF. In Fig. 7(d), this wavelength separation is changed to $\sim$2.4 nm to accommodate $\sim$27-Gb/s BPSK signals. For the OOK signals, the eye diagram has five signal levels that correspond to the number of 1's in adjacent four bits. BPSK and QPSK signals, however, do not have as many intermediate levels as OOK signals. This is due to the fact that the multiplexing is vector addition of the fields, bit-mismatches (e.g., -1) could create a vector with opposite direction as the final desired output. For example, in 4-bit pattern search in BPSK signals, when two bits match (and the other two bits mismatch), the output level is $1+1-1-1=0$, as opposed to $1+1+0+0=2$ in OOK signals. While there is no phase information in OOK correlation, the correlation results of phase-modulated signals contain both amplitude and phase information. With direct detection, correlation peaks identify the matching of phase differences between symbols. Homodyne coherent detection can be used on the correlator output instead to better distinguish between the exact patterns on phase-encoded signals. The BPSK and QPSK correlation results at 20 GBd with coherent detection are shown in Fig. 7(e). Coherent detection is performed using Agilent's N4391A Optical Modulation Analyzer. Optical fields can be recovered using coherent detection, and thus, exact phase pattern matching can be realized.

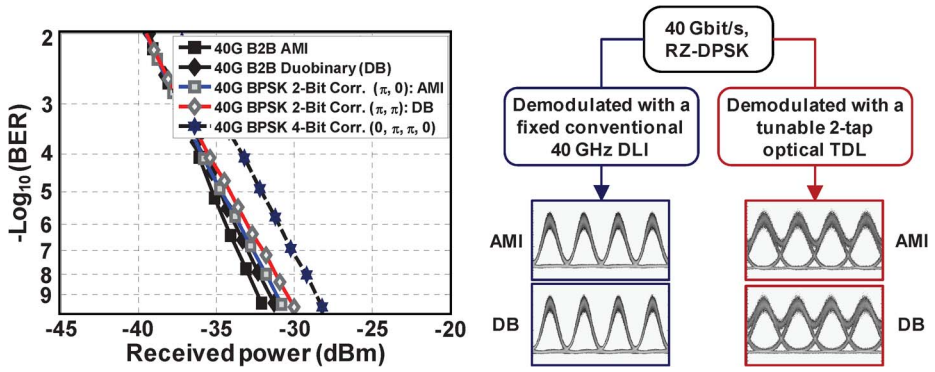

Fig. 8. All-optical correlation, BER performances: 4-bit BPSK pattern correlation, and 2-bit correlation (patterns "π 0" and "π π") resulting in differential demodulation of BPSK signal with the optical TDL, and comparison to conventional DLI DPSK demodulator performance. AMI: alternate mark inversion, DB: duobinary.

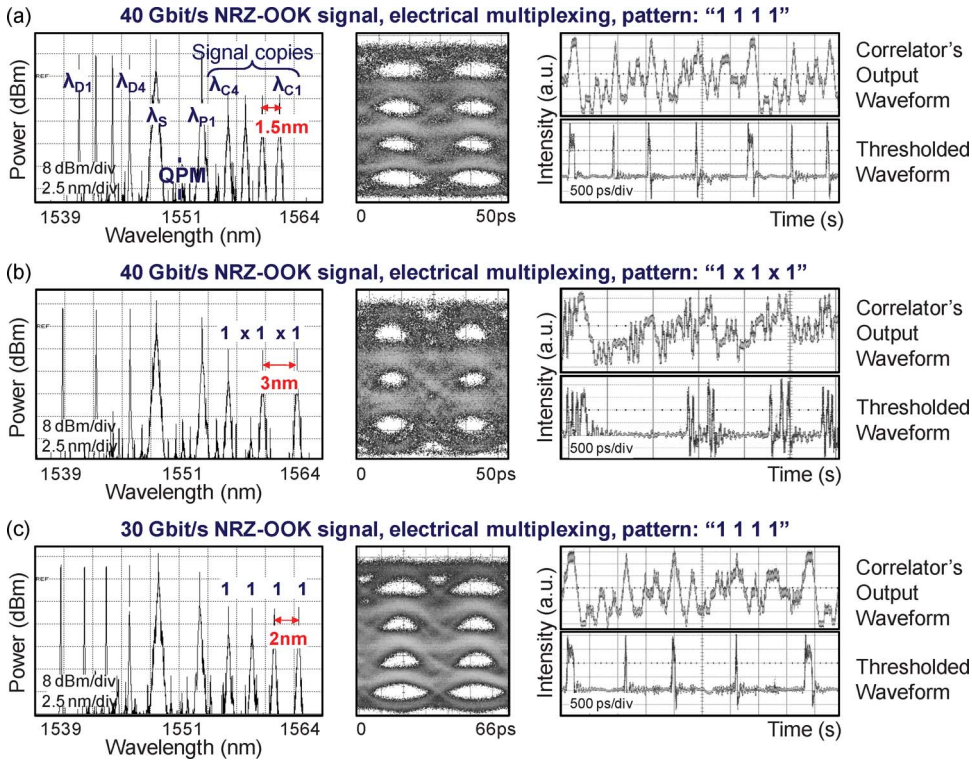

Fig. 9. Experimental results for the tunable correlator with electrical multiplexing. Nonlinear fan-out (multicasting) spectrum, correlator output eye diagram, correlator's output waveform, and electrically thresholded output waveform for (a) 40-Gb/s OOK pattern "1111", (b) 40-Gb/s OOK pattern "1 $\times$ 1 $\times$ 1", and (c) 30-Gb/s OOK pattern "1111". "$\times$" denotes a "don't care" bit.

A sample BER performance for the correlation of 4-bit pattern "0 π π 0" in a 40-Gb/s BPSK signal is given in Fig. 8. A special case of the correlator for BPSK signals is the 2-bit pattern search, which results in a delay-line interferometer (DLI) for differential detection. Correlation signal at λ_{MUX} can be set to the demodulated signals of alternate mark inversion (AMI) or duobinary (DB). In differential demodulation of BPSK signals using conventional DLI, AMI and DB signals are generated at the destructive and constructive ports of the interferometer, respectively. Therefore, a two-tap TDL with "π 0" tap phases can demodulate BPSK to AMI, and "π π" tap phases output a DB signal. We

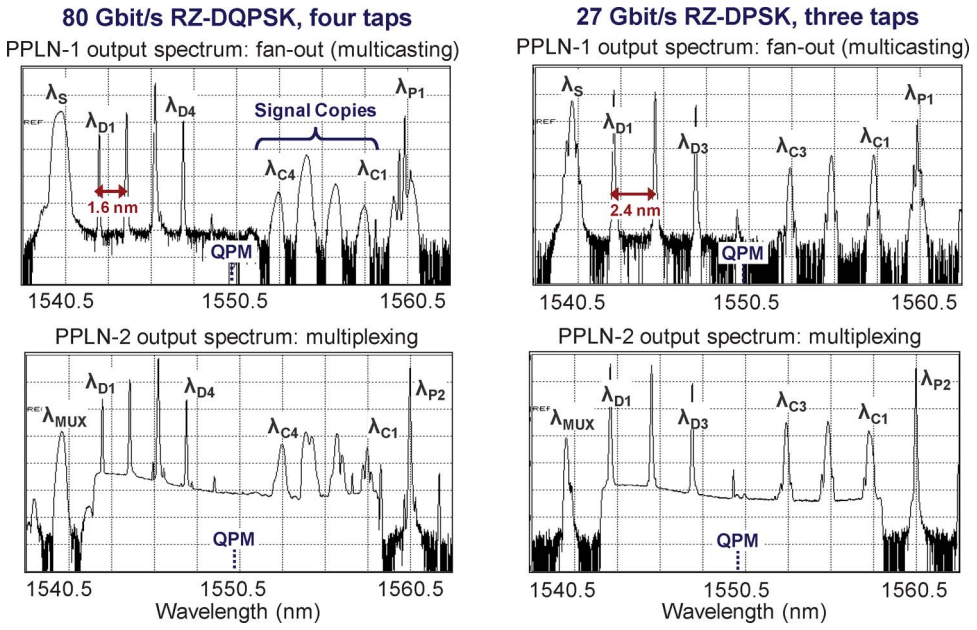

Fig. 10. Experimental spectra for different conditions of operation for the all-optical TDL equalizer, showing tunability to different bit rates and modulation formats.

demodulated the 40-Gb/s BPSK signal using the correlator. The BER results are shown in Fig. 8. When compared with the back-to-back performance (with a commercial 40-GHz DLI as the demodulator), the correlator outputs show 1-dB power penalty.

4.2. Correlation Using Electrical Multiplexing

If a photodiode is used to multiplex the taps, only intensity-modulated signals (OOK) can be used. Correlation results for the "1 1 1 1" sequence for a 40-Gb/s NRZ-OOK signal are given in Fig. 9(a). The wavelength spacing is set to ~1.5 nm to induce 25-ps delay after passing through ~1-km SMF with ~17-ps/nm/km dispersion. The correlation output waveform obtained with a photodiode is shown in Fig. 9(a), along with the corresponding eye diagram. The electrical thresholded waveform obtained with the thresholding receiver is also shown under the correlator pattern, identifying the occurrences of the "1 1 1 1" pattern. Correlation results for searching for a pattern with three 1 bits every other bit (pattern "1 *x* 1 *x* 1") at 40 Gb/s are also shown in Fig. 9(b). For further reconfigurability demonstration, the data rate is changed to 30 Gb/s, and $\Delta\lambda$ is tuned to ~2 nm in order to achieve ~33.3-ps delays to search for "1 1 1 1" pattern [see Fig. 9(c)].

5. Equalization of CD

Fiber CD distorts and broadens pulses in digital signals [1]. The TDL can be programmed to the inverse of the CD transfer function to "equalize" a distorted data stream by undoing the effect of pulse broadening [7]. Equalizers can significantly reduce the system penalties [1], [10]. Here, we demonstrate optical equalization using the optical TDL with optical and electrical multiplexing.

5.1. Optical TDL Equalizer With Optical Multiplexing

We implemented three- and four-tap optical TDLs to equalize for CD [33]. In a TDL equalizer, the tap spacing is usually set to half the symbol time of the digital signal [9].

Fig. 10 shows the spectra for the two nonlinear wave mixing stages (PPLN-1 and PPLN-2) of the TDL for equalization of a signal that is dispersed by 120-ps/nm dispersion. Fig. 10(a) shows the spectra for four-tap operation on a 40-GBd signal. The wavelength separation, $\Delta\lambda$, between the

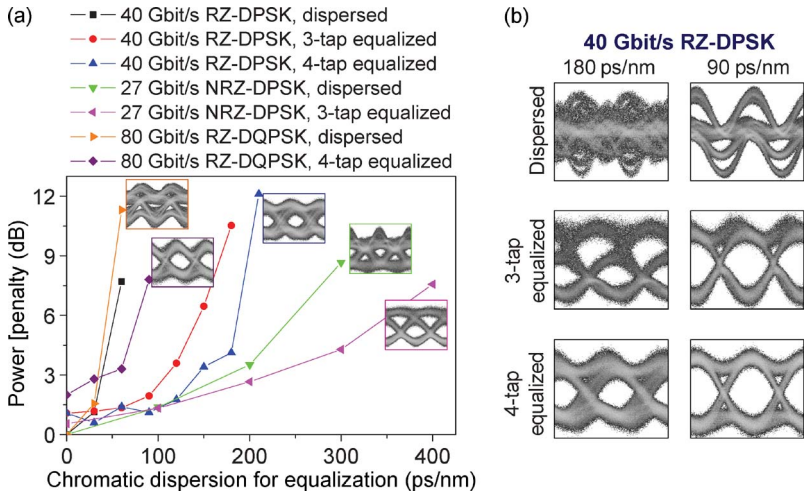

Fig. 11. (a) Measured power penalty at 10^{-9} BER versus CD applied on the input signal for equalization, demonstrating TDL reconfiguration to accommodate different bit rates and modulation formats. (b) Eye diagrams after direct detection in BPDs before and after equalization for three- and four-tap equalizers.

signal copies is set to ∼1.6 nm, which corresponds to a 12.5-ps delay after DCF. Therefore, half-symbol-time tap delays are achieved for the equalizer. In Fig. 10(b), the data are switched to ∼27-Gb/s DPSK. Thus, in order to achieve the half bit tap delays (∼18.8 ps), $\Delta\lambda$ is changed to ∼2.4 nm.

Bit error ratio (BER, i.e., the ratio of bit errors to total received bits) is measured before and after equalization for various CD values with direct detection. Received optical power required to achieve a BER value of 10^{-9} is measured for each modulation format at zero dispersion. For other values of dispersion, the additional optical power required to achieve the same 10^{-9} BER is known as power penalty and is measured in Fig. 11(a). Corresponding eye diagrams are also depicted for the end points of some of the curves. As can be seen, four-tap equalization results in improvements with respect to the three-tap equalization. The 40-Gb/s RZ-DPSK signal can tolerate ∼50-ps/nm CD before the power penalty exceeds 3 dB. This dispersion tolerance can be improved to ∼110 ps/nm and ∼160 ps/nm with three- and four-tap equalization, respectively. For 80-Gb/s RZ-DQPSK signal, the double wavelength conversion (0-ps/nm dispersion, single-tap operation) has an average penalty of ∼1.5 dB. Fig. 11(b) shows the eye diagrams of dispersed and TDL-equalized 40-Gb/s RZ-DPSK signals for 90-ps/nm and 180-ps/nm dispersion.

Experimental results on dispersion equalization on 80-Gb/s RZ-DQPSK signals using four taps (with half-symbol-time spacing) are shown in Fig. 12. Fig. 12(a) shows the BER curves versus received optical power. From Figs. 11(a) and 12(a), it can be observed that at 3-dB power penalty, the dispersion tolerance can be improved from ∼40 ps/nm to ∼70 ps/nm after TDL equalization. Fig. 12(b) depicts the eye diagrams of the dispersed and equalized signals. For dispersion values as high as 90 ps/nm, where the eye diagram is fully closed, a BER rate of 10^{-9} is achieved with 7.8-dB received power penalty. The equalized RZ signals in Fig. 12(b) seem degraded compared with the input signals, which might be the result of effects such as i) limited conversion bandwidth of the PPLN devices, ii) pulse broadening caused by the DCF in the TDL setup or the residual dispersion, and/or iii) degraded OSNR.

In this scheme, the number of taps for equalization is limited by the bandwidth of the intermediate devices (e.g., the nonlinear devices, optical amplifiers, etc.), the pump spacings, and maximum launch powers. Larger number of taps might be realized by adding pumps, cascading wave mixing stages, or using other frequency bands. Using a few taps would allow for suboptimal equalization [10].

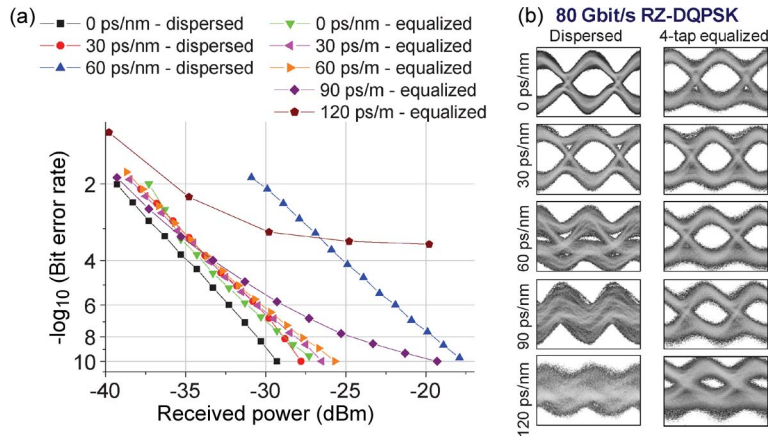

Fig. 12. (a) BER measurements on dispersed 80-Gb/s RZ-DQPSK signals before and after equalization using the all-optical TDL. (b) Eye diagrams of dispersed signal before and after equalization for 80-Gb/s RZ-DQPSK signal.

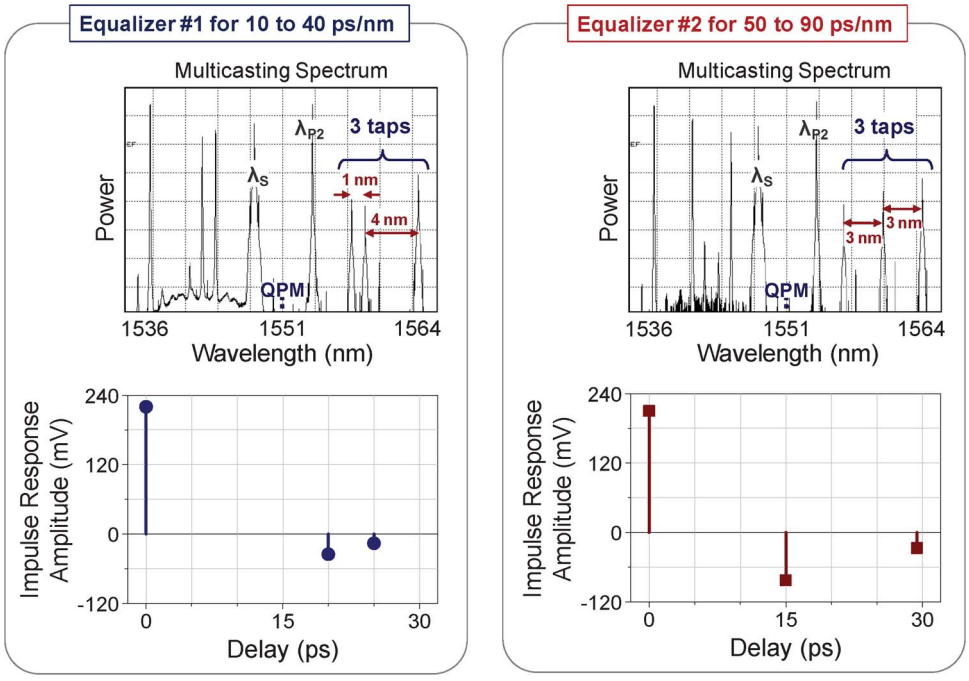

Fig. 13. TDL equalizer with electrical multiplexing. Multicasting spectra (top) for two equalizers with uniform and nonuniform tap spacing, along with plots of measured tap coefficients versus tap delays (bottom). Equalizers #1 and #2 are used to compensate 0–40-ps/nm and 50–90-ps/nm CD, respectively.

5.2. Optical TDL Equalizer With Electrical Multiplexing

A reconfigurable three-tap equalizer is demonstrated for equalization of a dispersed signal prior to detection. Two different equalizers are used for equalization of dispersion values from 0 to 40 ps/nm (equalizer #1), and dispersions of 50–90 ps/nm (equalizer #2). The multicasting spectra and the bipolar tap coefficients are shown in Fig. 13 for these two equalizers. For equalization of $0 - 40$ ps/nm, the second and the third pump lasers are set $\sim$4 nm and $\sim$5 nm away from the first pump to achieve delays of $\sim$20 ps and $\sim$25 ps, respectively. The delays were reconfigured to 15 and 29.5 ps by using

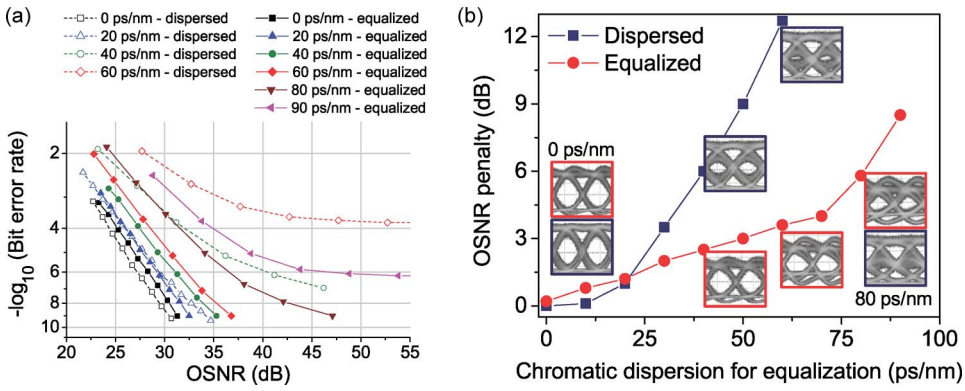

Fig. 14. (a) BER measurements of the dispersed back-to-back signal and after TDL equalization with electrical multiplexing. (b) OSNR penalty at 10^{-3} BER and corresponding eye diagrams for the equalized and dispersed signals.

~3-nm and ~6-nm separations from the first tap signal at $\lambda_{C1} \sim 1563$ nm. Fig. 14(a) shows the BER measurement results on the dispersed back-to-back signals and on the equalized signals. The OSNR penalty for dispersed and equalized signals at a BER of 10^{-3} are measured and shown in Fig. 14(b) along with corresponding eye diagrams at high OSNRs. A BER of 10^{-9} is still achievable using the equalizer for a residual dispersion of up to 80 ps/nm. There is ~60% improvement of dispersion tolerance at a 3-dB OSNR penalty.

6. Conclusion

We have demonstrated an optical TDL that utilizes nonlinear wave mixing and the frequency dependence of the speed of light to achieve tunability and reconfigurability of all parameters of the TDL. This optical TDL uses cascaded SFG and DFG mixings in a PPLN waveguide to produce variable-amplitude signal copies (taps) and conversion–dispersion-based optical delays to realize the tap delays. Therefore, the tap coefficients and the number of taps can be varied by changing the powers and wavelengths of the pumps used for wave mixing. Optical and electrical multiplexing of the taps have been shown. If optical multiplexing is used, complex tap coefficients can be realized by reusing the multicasting dummy laser pumps in the multiplexing nonlinear stage. Electrical multiplexing of the taps is also demonstrated with bipolar tap coefficients. The optical TDL was used to demonstrate correlation (pattern search) and equalization for CD at the speed of the line rate (80 Gb/s). Reconfigurablity of the TDL is further investigated in correlation and equalization on optical phase- and amplitude-modulated signals, where various patterns (0/1 intensity patterns, two- and four-phase-level patterns), different modulation formats (OOK, BPSK, and QPSK), and different line rates (27/40/80 Gb/s) are demonstrated.

References

[1] G. Agrawal, *Nonlinear Fiber Optics*. San Diego, CA: Academic, 2001.
[2] J. Leuthold, C. Koos, and W. Freude, "Nonlinear silicon photonics," *Nat. Photon.*, vol. 4, no. 8, pp. 535–544, Aug. 2010.
[3] G. Steinmeyer, D. H. Sutter, L. Gallmann, N. Matuschek, and U. Keller, "Frontiers in ultrashort pulse generation: Pushing the limits in linear and nonlinear optics," *Science*, vol. 286, no. 5444, pp. 1507–1512, Nov. 1999.
[4] J. Kakande, R. Slavík, F. Parmigiani, A. Bogris, D. Syvridis, L. Grüner-Nielsen, R. Phelan, P. Petropoulos, and D. J. Richardson, "Multilevel quantization of optical phase in a novel coherent parametric mixer architecture," *Nat. Photon.*, vol. 5, no. 12, pp. 748–752, Dec. 2011.
[5] H. Hu, E. Palushani, M. Galili, H. C. H. Mulvad, A. Clausen, L. K. Oxenløwe, and P. Jeppesen, "640 Gbit/s and 1.28 Tbit/s polarisation insensitive all optical wavelength conversion," *Opt. Exp.*, vol. 18, no. 10, pp. 9961–9966, May 2010.
[6] A. Bogoni, X. Wu, S. R. Nuccio, J. Wang, Z. Bakhtiari, and A. E. Willner, "Photonic 640-Gb/s reconfigurable OTDM add–drop multiplexer based on pump depletion in a single PPLN waveguide," *IEEE J. Sel. Topics Quantum Electron.*, vol. 18, no. 2, pp. 709–716, Mar./Apr. 2012.
[7] J. G. Proakis, *Digital Communications*. New York: McGraw-Hill, 2000.

[8] M. C. Hauer, J. E. McGeehan, S. Kumar, J. Touch, J. Bannister, E. R. Lyons, C. H. Lin, A. A. Au, H. P. Lee, D. S. Starodubov, and A. E. Willner, "Optically-assisted internet routing using arrays of novel dynamically reconfigurable FBG-based correlators," *IEEE J. Lightw. Technol.*, vol. 21, no. 11, pp. 2765–2778, Nov. 2003.
[9] J. K. Fischer, R. Ludwig, L. Molle, C. Schmidt-Langhorst, C. C. Leonhardt, A. Matiss, and C. Schubert, "High-speed digital coherent receiver based on parallel optical sampling," *IEEE J. Lightw. Technol.*, vol. 29, no. 4, pp. 378–385, Feb. 2011.
[10] C. R. Doerr, S. Chandrasekhar, P. J. Winzer, A. R. Chraplyvy, A. H. Gnauck, L. W. Stulz, R. Pafchek, and E. Burrows, "Simple multichannel optical equalizer mitigating intersymbol interference for 40-Gb/s nonreturn-to-zero signals," *IEEE J. Lightw. Technol.*, vol. 22, no. 1, pp. 249–256, Jan. 2004.
[11] H. J. Caulfield and S. Dolev, "Why future supercomputing requires optics," *Nat. Photon.*, vol. 4, no. 5, pp. 261–263, May 2010.
[12] B. Moslehi, J. W. Goodman, M. Tur, and H. J. Shaw, "Fiber-optic lattice signal processing," *Proc. IEEE*, vol. 72, no. 7, pp. 909–930, Jul. 1984.
[13] M. S. Rasras, I. Kang, M. Dinu, J. Jaques, N. Dutta, A. Piccirilli, M. A. Cappuzzo, E. Y. Chen, L. T. Gomez, A. Wong-Foy, S. Cabot, G. S. Johnson, L. Buhl, and S. S. Patel, "A programmable 8-bit optical correlator filter for optical bit pattern recognition," *IEEE Photon. Technol. Lett.*, vol. 20, no. 9, pp. 694–696, May 2008.
[14] J. Capmany and D. Novak, "Microwave photonics combines two worlds," *Nat. Photon.*, vol. 1, no. 6, pp. 319–330, Jun. 2007.
[15] J. Yao, "Microwave photonics," *IEEE J. Lightw. Technol.*, vol. 27, no. 3, pp. 314–335, Feb. 2009.
[16] J. Sharping, Y. Okawachi, J. van Howe, C. Xu, Y. Wang, A. Willner, and A. Gaeta, "All-optical, wavelength and bandwidth preserving, pulse delay based on parametric wavelength conversion and dispersion," *Opt. Exp.*, vol. 13, no. 20, pp. 7872–7877, Oct. 2005.
[17] G. Contestabile, M. Presi, and E. Ciaramella, "Multiple wavelength conversion for WDM multicasting by FWM in an SOA," *IEEE Photon. Technol. Lett.*, vol. 16, no. 7, pp. 1775–1777, Jul. 2004.
[18] C.-S. Bres, N. Alic, E. Myslivets, and S. Radic, "Scalable multicasting in one-pump parametric amplifier," *IEEE J. Lightw. Technol.*, vol. 27, no. 3, pp. 356–363, Feb. 2009.
[19] A. Biberman, B. G. Lee, A. C. Turner-Foster, M. A. Foster, M. Lipson, A. L. Gaeta, and K. Bergman, "Wavelength multicasting in silicon photonic nanowires," *Opt. Exp.*, vol. 18, no. 17, pp. 18 047–18 055, Aug. 2010.
[20] J. Wang, J. Sun, X. Zhang, D. Huang, and M. M. Fejer, "Optical phase erasure and its application to format conversion through cascaded second-order processes in periodically poled lithium niobate," *Opt. Lett.*, vol. 33, no. 16, pp. 1804–1806, Aug. 2008.
[21] T. Kurosu and S. Namiki, "Continuously tunable 22 ns delay for wideband optical signals using a parametric delay-dispersion tuner," *Opt. Lett.*, vol. 34, no. 9, pp. 1441–1443, May 2009.
[22] N. Alic, J. R. Windmiller, J. B. Coles, S. Moro, E. Myslivets, R. E. Saperstein, J. M. C. Boggio, C. S. Bres, and S. Radic, "105-ns continuously tunable delay of 10-Gb/s optical signal," *IEEE Photon. Technol. Lett.*, vol. 20, no. 13, pp. 1187–1189, Jul. 2008.
[23] L. Christen, O. F. Yilmaz, S. Nuccio, X. Wu, I. Fazal, A. E. Willner, C. Langrock, and M. M. Fejer, "Tunable 105 ns optical delay for 80 Gb/s RZ-DQPSK, 40 Gb/s RZ-DPSK, and 40 Gb/s RZ-OOK signals using wavelength conversion and chromatic dispersion," *Opt. Lett.*, vol. 34, no. 4, pp. 542–544, Feb. 2009.
[24] S. R. Nuccio, O. F. Yilmaz, X. Wu, and A. E. Willner, "Fine tuning of conversion/dispersion based optical delays with a 1 pm tunable laser using cascaded acousto-optic mixing," *Opt. Lett.*, vol. 35, no. 4, pp. 523–525, Feb. 2010.
[25] E. J. M. Verdurmen, G. D. Khoe, A. M. J. Koonen, and H. deWaardt, "All optical data format conversion from WDM to OTDM based on FWM," *Microw. Opt. Technol. Lett.*, vol. 48, no. 5, pp. 992–994, May 2006.
[26] X. Wu, A. Bogoni, S. R. Nuccio, O. F. Yilmaz, M. Scaffardi, and A. E. Willner, "High-speed optical WDM-to-TDM conversion using fiber nonlinearities," *IEEE J. Sel. Topics Quant. Electron.*, vol. 16, no. 5, pp. 1441–1447, Sep./Oct. 2010.
[27] H. Sotobayashi, W. Chujo, and K. Kitayama, "Photonic gateway: TDM-to-WDM-to-TDM conversion and reconversion at 40 Gbit/s (4 channels$\times$ 10 Gbits/s)," *J. Opt. Soc. Amer. B, Opt. Phys.*, vol. 10, no. 11, pp. 2810–2816, Nov. 2002.
[28] T. Ohara, H. Takara, I. Shake, K. Mori, S. Kawanishi, S. Mino, T. Yamada, M. Ishii, T. Kitoh, T. Kitagawa, K. R. Parameswaran, and M. M. Fejer, "160-Gb/s optical-time-division multiplexing with PPLN hybrid integrated planar lightwave circuit," *IEEE Photon. Technol. Lett.*, vol. 15, no. 2, pp. 302–304, Feb. 2003.
[29] C. Langrock, S. Kumar, J. E. McGeehan, A. E. Willner, and M. M. Fejer, "All-optical signal processing using χ^2 nonlinearities in guided-wave devices," *IEEE J. Lightw. Technol.*, vol. 24, no. 7, pp. 2579–2592, Jul. 2006.
[30] S. Frisken, G. Baxter, D. Abakoumov, H. Zhou, I. Clarke, and S. Poole, "Flexible and grid-less wavelength selective switch using LCOS Technology," in *Proc. OFC*, 2011, pp. OTuM3-1–OTuM3-3.
[31] O. F. Yilmaz, S. Khaleghi, N. Ahmed, S. R. Nuccio, I. M. Fazal, X. Wu, and A. E. Willner, "Reconfigurable and finely tunable optical tapped-delay-line to achieve 40 Gb/s equalization and correlation using conversion/dispersion based delays," in *Proc. ECOC*, 2010, p. Mo.2.A.2.
[32] O. F. Yilmaz, S. Khaleghi, M. R. Chitgarha, S. R. Nuccio, and A. Willner, "Demonstration of 28–40-Gbaud, OOK/BPSK/QPSK data-transparent optical correlation with control/tunability over time delays, phases and number of taps," in *Proc. OFC*, 2011, pp. OThN1-1–OThN1-3.
[33] S. Khaleghi, O. F. Yilmaz, M. R. Chitgarha, I. M. Fazal, and A. Willner, "80-Gbit/s DQPSK optical tapped-delay-line equalization using finely tunable delays, phases and amplitudes," in *Proc. OFC*, 2011, pp. OThN4-1–OThN4-3.